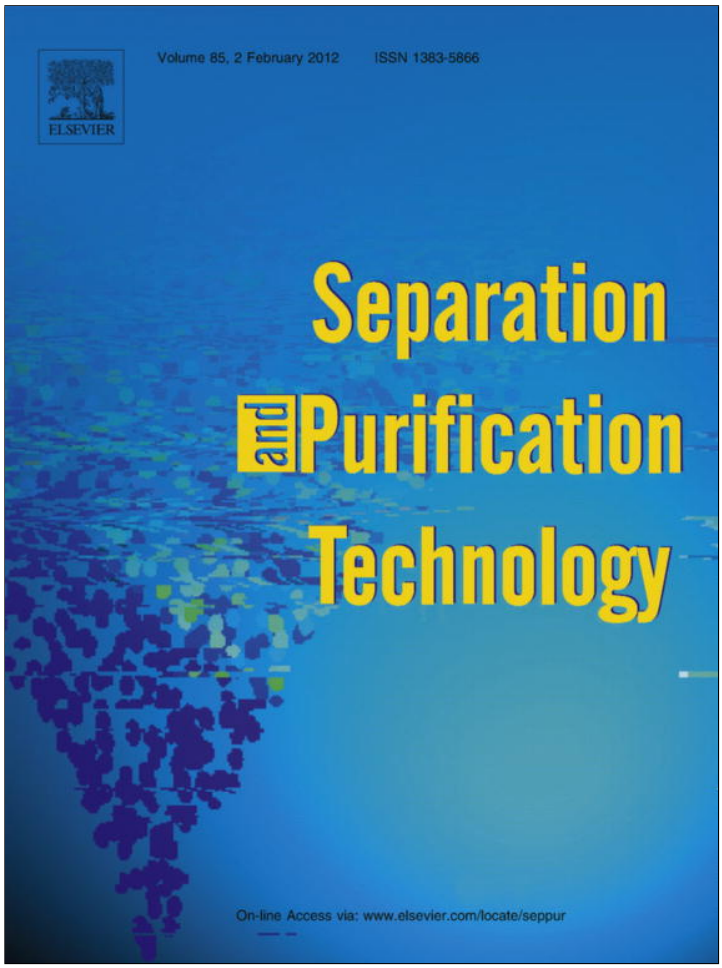

(This is a sample cover image for this issue. The actual cover is not yet available at this time.)

Separation and Purification Technology 103 (2013) 78–83

Contents lists available at SciVerse ScienceDirect

Separation and Purification Technology

journal homepage: www.elsevier.com/locate/seppur

Effect of graphite oxide and multi-walled carbon nanotubes on the microstructure and performance of PVDF membranes

Yufen Zhao [a], Zhiwei Xu [a,*], Mingjing Shan [a], Chunying Min [b], Baoming Zhou [a], Yinglin Li [a], Baodong Li [a], Liangsen Liu [a], Xiaoming Qian [a]

[a] State Key Laboratory of Hollow Fiber Membrane Materials and Processes, School of Textiles, Tianjin Polytechnic University, Tianjin 300387, People's Republic of China
[b] School of Material Science and Engineering, Jiangsu University, Zhenjiang 212013, People's Republic of China

ARTICLE INFO

Article history:
Received 20 June 2012
Received in revised form 2 October 2012
Accepted 6 October 2012
Available online 23 October 2012

Keywords:
Blend ultrafiltration membranes
Multi-walled carbon nanotubes
Graphite oxide
Microstructure
Hydrophilicity

ABSTRACT

Polyvinylidene fluoride (PVDF)/graphite oxide (GO) and PVDF/multi-walled carbon nanotubes (MWCNTs) ultrafiltration membranes were prepared by solution-blending the ternary mixture of PVDF/carbon materials/dimethylacetamide in combination of the phase inversion method. It was indicated that the blend membranes exhibit better pore structure and higher surface roughness than the pristine ones, and PVDF/GO blend membranes contributed bigger pores but lower surface roughness than PVDF/MWCNTs blend membranes. For PVDF/MWCNTs and PVDF/GO blend membranes, 114% and 74% improvement of pure water permeation flux was achieved, respectively. The hydrophilicity was increased significantly and the bovine serum albumin rejection of PVDF/MWCNTs and PVDF/GO blend membranes was enhanced about 31.8% and 28.7%, respectively, compared with those of the pure PVDF membranes. Hence, it can be expected that graphitic carbon materials open up a new pathway for improving the performance of blend membranes and the ultrafiltration membranes modified by graphitic carbon materials have a promising application prospect.

1. Introduction

The preparation of organic–inorganic composite membranes [1–4] has been a point of considerable interest over the last decades. And the presence of finely dispersed inorganic particles in a polymer matrix has proven very useful in the improvement of membrane performance for separation processes, especially in the waste water treatment field, including oil–water [5–7] and protein effluent separation [8,9]. The hydrophilicity of membranes and their porous structure play important roles in membrane-separation processes. An appropriate porous membrane must have high permeability, good hydrophilicity, and excellent chemical resistance to the feed streams. In order to obtain high permeability, membranes should have high surface porosity and good pore structure. Polyvinylidene fluoride (PVDF) is a common ultrafiltration, microfiltration and pervaporation membrane material because of its excellent chemical resistance and thermal stability. However, its super hydrophobicity limits its applications in membrane separation process. Many studies have attempted to change the membrane porous structure and enhance the hydrophilicity of PVDF membranes by adding inorganic particles such as Al_2O_3 [10,11], SiO_2 [12,13], TiO_2 [14–16], ZrO_2 [17], Fe_3O_4 [18] and $LiClO_4$ [19]. It has been demonstrated that the addition of inorganic filler has led to an increase in the membrane permeability and an effective domination of membrane surface architecture [10–19]. But there were no oxygen-containing functional groups on the surface of inorganic materials that are mainly used in previous studies. As a result, the common feature of these modifications was the addition of a high proportion of inorganic materials, such as SiO_2–PVDF [13], ZrO_2–PVDF [17], and $LiClO_4$–PVDF [19] membranes with ratios of inorganic particles to PVDF of 0.1, 1.0, and 0.128, respectively. And the morphology and elasticity of PVDF blend membranes were both significantly affected by the mass of inorganic materials added. In this regard, it is of tremendous importance to search and identify the (inorganic) materials that not only improve the hydrophilic character of membrane but also enhance the permeability of membrane by adding a small fraction.

Recently, the application of graphitic carbon materials for preparing ultrafiltration membranes has attracted considerable attention. Multi-walled carbon nanotubes (MWCNTs) possess much higher specific surface compared with the mainly used three-dimensional materials in previous studies. MWCNTs are also one of candidates to create a surface with a roughness at mirco/nanometer level owing to their rigid cylindrical nanostructures with a diameter ranging from about 1 nm to dozens of nanometers and length ranging from hundreds of nanometers to micrometers, which could lead to the increase of efficient filtration area and permeability of blend membranes. There are some studies on

* Corresponding author. Tel./fax: +86 022 83955231.
E-mail address: xuzhiwei@tjpu.edu.cn (Z. Xu).

1383-5866/$ - see front matter © 2012 Published by Elsevier B.V.
http://dx.doi.org/10.1016/j.seppur.2012.10.012

MWCNTs/organic hybrid membranes [20–29], which have been shown to have higher water fluxes and protein rejection rates compared with pure membranes. Choi et al. [23] prepared MWCNT-blended membranes via the phase inversion method. The addition of MWCNTs alleviated the membrane fouling caused by natural water. Gao et al. [29] found that the treated MWCNTs displayed excellent compatibilities with the polymeric components of blend membranes. Another potential candidate to effectively modify polymeric materials is graphite [30]. It has an exceptionally high strength and stiffness in combination with easy functionalization. Nonetheless, graphite is chemically inert and can not be dissolved in typical organic solvents. As an affinity of graphite, graphite oxide (GO) with the carboxylic and hydroxy groups is suitable for preparing organic–inorganic blend ultrafiltration membranes. GO is a layered material containing oxygen functional groups on its basal planes and edges. Because of the reactive surface sites and layered structure of GO, it may provide potential nanoscale building blocks for new materials for the synthesis of GO-containing nanocomposites. It has been demonstrated that GO nanocomposites exhibit high mechanical strength combined with exciting physical properties [31–34]. Therefore, it is expected that MWCNTs and GO would improve the hydrophilicity and permeability of PVDF membranes. However, the influence of these graphitic carbon materials on the microstructure and performance of PVDF membranes has not been reported.

In the present study, PVDF blend ultrafiltration membranes were prepared by adding a small fraction of graphitic carbon materials with the phase inversion method. The objective of this work was to systematically reveal the morphology, hydrophilicity and permeability of the PVDF/graphitic carbon material blend membranes. Then a series of experiments, such as water contact angle (CA), water flux, bovine serum albumin (BSA) rejection and porosity measurements, scanning electron microscopy (SEM) and atomic force microscopy (AFM) analysis, were carried out for membrane characterization.

2. Experimental

2.1. Materials

PVDF (FR901) was purchased from Shanghai 3F New Materials Co. Ltd., China. N,N-dimethylacetamide (DMAc, >99.5%, reagent) was purchased from Tianjin Weichen Chemical Reagent Co. Ltd., China. MWCNTs (with diameters of 10–50 nm and length of 1–30 μm) were obtained from Nanjing XF Nanomaterial Science and Technology Co. Ltd., and were purified with sulphuric acid. Graphite was purchased from the Qingdao Ruisheng Graphite Co. Ltd., China. The other additive was polyvinyl pyrrolidone (PVP). The distilled water was used as the nonsolvent for the polymer precipitation.

2.2. Preparation of GO

GO was prepared by the improved Hummers' method [35]. A 9:1 mixture of concentrated H_2SO_4/H_3PO_4 (360:40 mL) was added to a mixture of 3.0 g graphite flakes and 18.0 g $KMnO_4$, producing a slight exotherm to 35–40 °C. The reaction was then heated to 50 °C and stirred for 12 h. The reactants were cooled to room temperature and poured onto ice (~400 mL). The mixture was centrifuged and the supernatant was decanted away. The remaining solid material (GO) was rinsed repeatedly in deionized water until the pH of the solution reached approximately 7.0, and then it was dried in a vacuum oven at 50 °C.

2.3. Membrane preparation

Cast solutions were prepared using following steps by the phase inversion method, MWCNTs (1%, percentage of PVDF weight) were dissolved into DMAc (78%, by weight of the solution) in an ultrasonic bath for at least 2 h, which facilitated the dispersion of the MWCNTs. PVDF (19%, by weight of the solution) and PVP (3%, by weight of the solution) were then added into the solution followed by an 24 h stirring at 40 °C [10]. At the end of the mixing process all the polymers were convincingly dissolved.

In this research, PVP was used to enhance the porosity of PVDF membrane [36], and it might increase membrane hydrophilicity due to the residue trapped in the membrane matrix [37]. Therefore, to highlight the special contribution of graphitic carbon materials in hydrophilicity and permeability, a pure membrane was fabricated as a control by proper over-dosage of PVP (3% PVP, by weight of the solution, determined after several tests).

For the membranes of PVDF/GO, the concentration of GO was the same as that of MWCNTs in the casting solutions. The casting solution of pure PVDF membrane was prepared by dissolving 19 g PVDF and 3 g PVP in 78 g DMAc. After releasing the bubbles in vacuum oven, the homogeneous casting solution was spread into liquid film on a glass plate with a steel knife, and then the solution films were immediately immersed in a coagulation bath of distilled water (25 °C). The formed membranes were peeled off and subsequently washed with distilled water to remove residual solvent. After being thoroughly dried, the membranes were used as samples for characterization. The residual membranes were kept in distilled water for filtration tests.

2.4. Characterization of membranes

The permeation flux and rejection of the membranes were measured by ultrafiltration experimental equipment. The rejection tests were carried out with an aqueous solution of BSA (molecular weight = 67,000) (1 g L^{-1}). All experiments were conducted at 25 °C and under the feed pressure of 0.1 MPa. The newly prepared flat-sheet membranes were pre-pressured at 0.1 MPa using the pure water for 1 h before measurement, and then the pure water permeation and rejection for the BSA solution were measured. The concentrations of BSA in the permeation and feed solution were determined by an UV-spectrophotometer (Shimadzu UV-2450, Japan). The permeation flux and rejection were defined as formulae (1) and (2), respectively.

$$J = \frac{Q}{A \times T} \tag{1}$$

$$R = \left(1 - \frac{C_P}{C_F}\right) \times 100\% \tag{2}$$

where J was the permeation flux of membrane for pure water (L m^{-2} h^{-1}), Q was the volume of permeate pure water (L), A was the effective area of membrane (m^2) and T was the permeation time (h). R was the rejection to BSA (%). C_P and C_F were the concentrations of BSA in the permeate and feed solution, respectively (wt%).

The membrane porosity ε (%) was defined as the volume of pores divided by the total volume of porous membrane. It could usually be determined by gravimetric method, determining the weight of liquid (here pure water) contained in the membrane pores [38].

$$\varepsilon = \frac{(w_1 - w_2)/d_w}{(w_1 - w_2)/d_w + w_2/d_p} \times 100\% \tag{3}$$

where w_1 was the weight of the wet membrane (g), w_2 was the weight of the dry membrane (g), d_w was the pure water density (0.998 g cm^{-3}) and d_p was the polymer density (as the inorganic

content in the membrane matrix was small and d_p was approximate to d_{PVDF}, namely 1.765 g cm^{-3}).

The CA between water and the membrane surface was measured with a contact-angle measurement apparatus (JYSP-180 Contact Angle Analizer) according to the sessile-drop method. Briefly, a water droplet was deposited on a flat homogeneous membrane surface and the contact angle of the droplet with the surface was measured. The value was observed until there was no change in CA during the short measurement period. Each CA was measured five times at five different points of each membrane sample and an average value was calculated.

The surface and cross-sectional structures of the membranes were examined by SEM (Quanta 200, Holland). Cross-sections were prepared by fracturing the membranes at the temperature of liquid nitrogen. All specimens were coated with a thin layer of gold before being observed using SEM. AFM (CSPM5500) was employed to analyze the surface morphology and roughness of the membranes. In the range of the scan areas 10 μm × 10 μm, roughness parameters could also be obtained with the AFM analysis software, and small squares of the prepared membranes (approximately 1 cm^2) were cut and glued on the glass substrate before being scanned (10 μm × 10 μm). Fourier-transform infrared spectroscopy (FTIR) was used to identify functional groups on the surface of MWCNTs and GO. The pore density and average pore size of membranes were measured by professional image analysis method.

3. Results and discussion

3.1. Characterization of MWCNTs and GO

A difference between FTIR spectra of MWCNTs and GO was shown in Fig. 1. The peaks emerging at 1400, 1620, 1730, and 3100–3600 cm^{-1} were corresponded to C=C, C=O, COOH and O—H bonds, and the results were in good agreement with the results of previous reports [39,40]. Fig. 1a shows the FTIR spectrum of MWCNTs, and it was seen that the MWCNTs have less functional groups than GO. The appearance of peaks at 1400, 1620 and 3440 cm^{-1} is attributed to C=O, C=C and O—H bond of MWCNTs and GO, respectively. A new peak at 1730 cm^{-1} of GO indicates the presence of carboxyl groups (Fig. 1b). The higher intensity of band at 3100–3600 cm^{-1} for GO compared with MWCNTs was due to the hydroxyl stretching vibration of the carboxylic group (COOH). Generally, these oxygen-containing functional groups on the MWCNTs and GO would be beneficial to the improvement of membrane hydrophilicity. Meanwhile, the hydrophily of functional groups improves the dispersibility of MWCNTs and GO in aqueous solution.

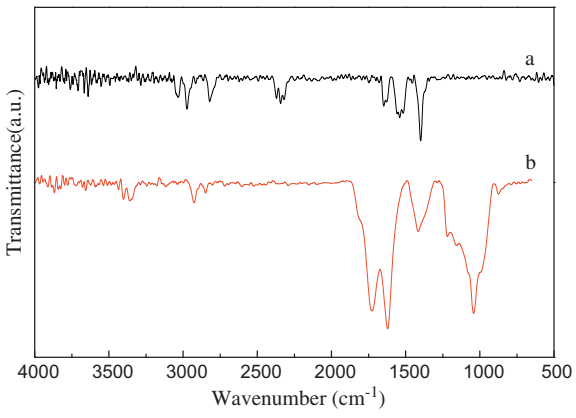

Fig. 1. FTIR spectra of MWCNT and GO.

3.2. Microstructures of membranes

SEM and AFM analysis was performed to compare the morphological changes between pristine and blend membranes. Fig. 2 shows SEM micrographs of the surface, cross-section, and inner structures of PVDF, PVDF/GO and PVDF/MWCNTs membranes. Comparing the pristine and blend membranes, the minor variation of membrane pores in number and size was observed, which was also reflected by the pore density and average pore size shown in Fig. 3. Obviously, the blend membranes displayed better surface morphology than pristine membranes, and PVDF/GO blend membranes have bigger pores but lower pore density than PVDF/MWCNTs blend membranes (shown in Fig. 2b and c). The difference could be interpreted as follows. GO was a kind of hydrophilic material because of the rich oxygen-containing functional groups. During the membrane preparation process, the diffusion rate between gels (water) and solvent (DMAc) could be accelerated by GO. The occurrence of phase separation process, which was good for the generation of polymer-poor phase, was also facilitated by the presence of GO in membrane preparation process. Therefore, larger pore channels would form due to the rapid mass transformation. In contrast, the MWCNTs had weaker effects for this exchange rate between solvent and non-solvent during the membrane formation due to less oxygen-containing functional groups on the surface compared with GO. However, the appearance of MWCNTs to the surface of PVDF/MWCNTs membranes was obvious when the surface photographs of prepared membranes were compared as presented in Fig. 2c, which may be related to increase hydrophilicity of membrane.

It can be seen that all of the membranes showed a typical asymmetric porous structure with a skin layer and a finger-like porous sublayer. The finger-like pores for all of the blended membranes were much wider than those of the PVDF membrane (Fig. 2d–f). These results indicated that the addition of graphitic carbon materials plays an important role in the membrane formation process due to the surface properties of MWCNTs and GO such as surface charge, surface functional groups and active site concentrations, to such an extent as to modify the membrane microstructure. The Fig. 2g–i shows the inner structures of membranes, and indicates that carbon materials remained well dispersed in the PVDF membranes. The pure PVDF and PVDF/MWCNTs blend membranes had a sponge-like cross-section but also presented some differences in compact morphologies. Nevertheless, the formation of sponge-like cross-section was suppressed by the addition of GO into the membrane structure. GO with many types of hydrophilic groups, increased the rapid mass transformation between the solvent and non-solvent during the phase inversion, resulting in forming the floppy inner cross-section. After the addition of MWCNTs, the cross-section became a little denser. The SEM images indicate that the addition of carbon materials greatly influenced the membrane structures, thereby altering the pore density and pore diameter of surface micropores.

Fig. 4 displays three-dimensional AFM images of the membrane surfaces. The surface roughness of blend membranes was apparently higher than that of prisitine membranes. There exists mean roughness (R_a), root mean square (R_q), and mean difference in the height between the five highest peaks and the five lowest valleys (R_z). The surface roughness of PVDF/carbon materials blend membranes was higher than that of pure PVDF membrane, and the roughness parameter (R_a) of PVDF/MWCNTs blend membranes was largest (shown in Table 1). High roughness commonly led to two changes in membranes: an increase of efficient filtration area and a decrease of the anti-fouling performance, and then the enlarged efficient filtration area increased the membrane flux directly [10]. Besides, the accumulation of two carbon materials on the membrane surface can increase the effective filtration area of

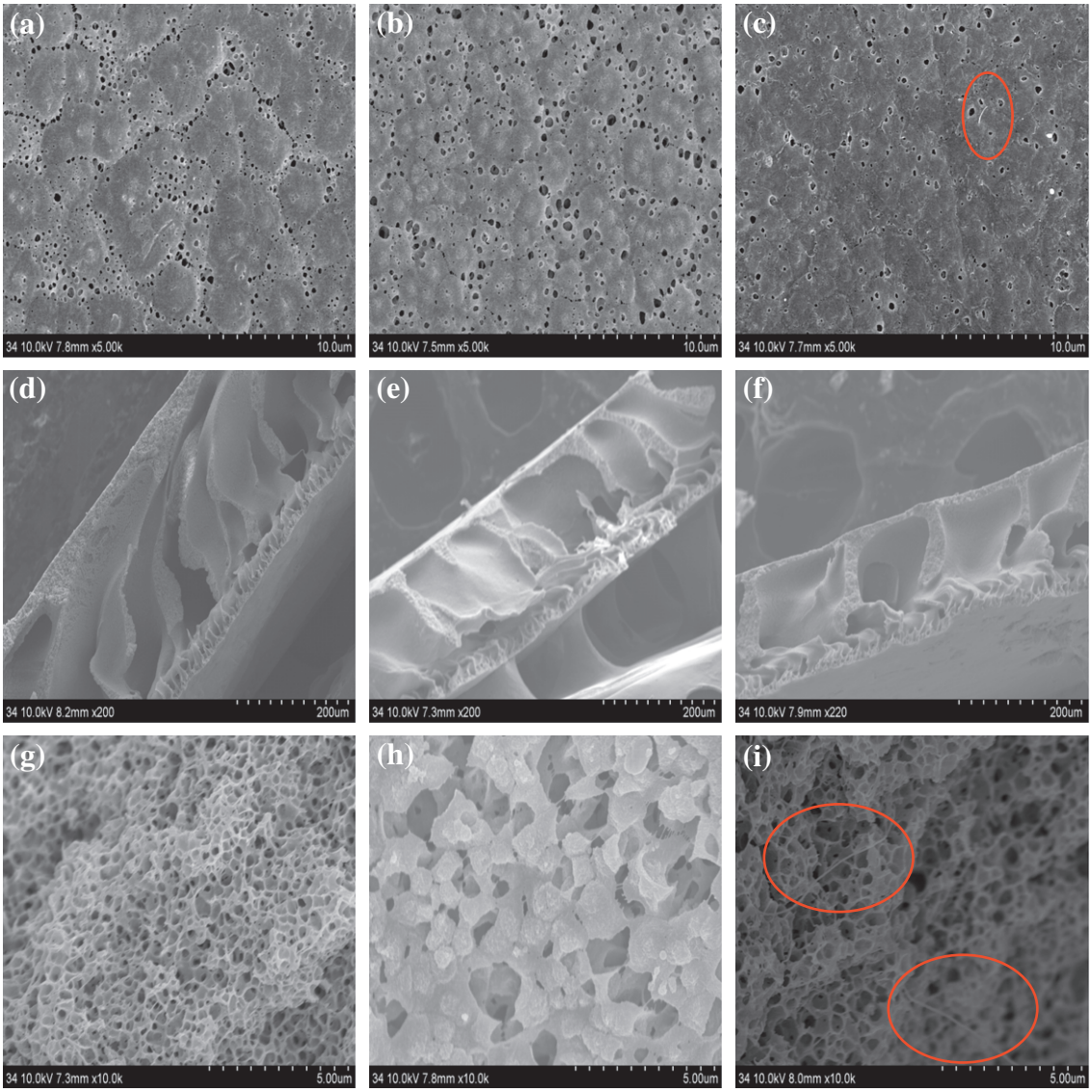

Fig. 2. SEM micrographs of PVDF membranes: (a), (b) and (c) represented surface of PVDF, PVDF/GO and PVDF/MWCNTs membranes. (d), (e) and (f) represented cross-section of PVDF, PVDF/GO and PVDF/MWCNTs membranes. (g), (h) and (i) represented inner porous structures of PVDF, PVDF/GO and PVDF/MWCNTs membranes.

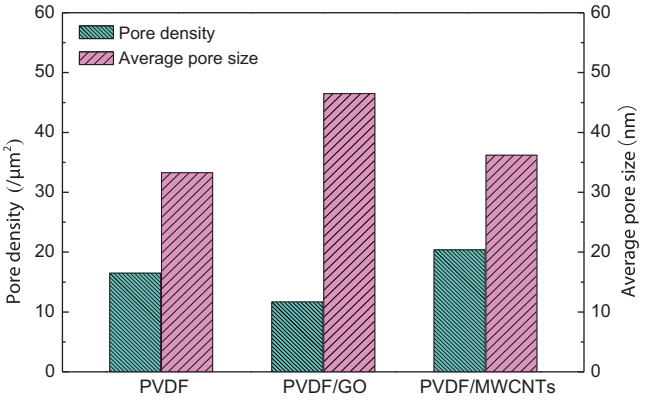

Fig. 3. Pores density and the average pore size of the membranes.

membrane ultimately. Consequently, it could be anticipated that the MWCNTs and GO have profound influences on the hydrophilicity and permeation of PVDF membranes.

3.3. Contact angle, porosity and rejection values of membranes

The contact angle is an important parameter for measuring surface hydrophilicity [41]. In general, a smaller contact angle corresponds to a more hydrophilic material. The contact angle data of three blend membranes were shown in Table 2. These results demonstrated that adding carbon materials to PVDF could improve its hydrophilicity. Table 2 shows the decrease in contact angle with the addition of MWCNTs and GO, which might play a favorable role in elevating the pure water flux of blend membranes. As it was shown in Fig. 2c, the nanotubes can be seen on the membrane surface, which may be related to the hydrophilicity increase of membranes. And this led to the more decrease in contact angle of PVDF/MWCNTs membrane than PVDF/GO membrane. In addition, as could be seen from Table 2, the porosity of PVDF/carbon material blend membranes was marginally higher than that of pure PVDF membrane. Considering about BSA rejection ratio, the results were also depicted in Table 2. The BSA rejection increased from 67.6% to 87.0% and 89.1% when the GO and MWCNTs were added, respectively. Generally, CNTs have exhibited the capability for the removal of albumin as a type of adsorbent [42]. Moreover,

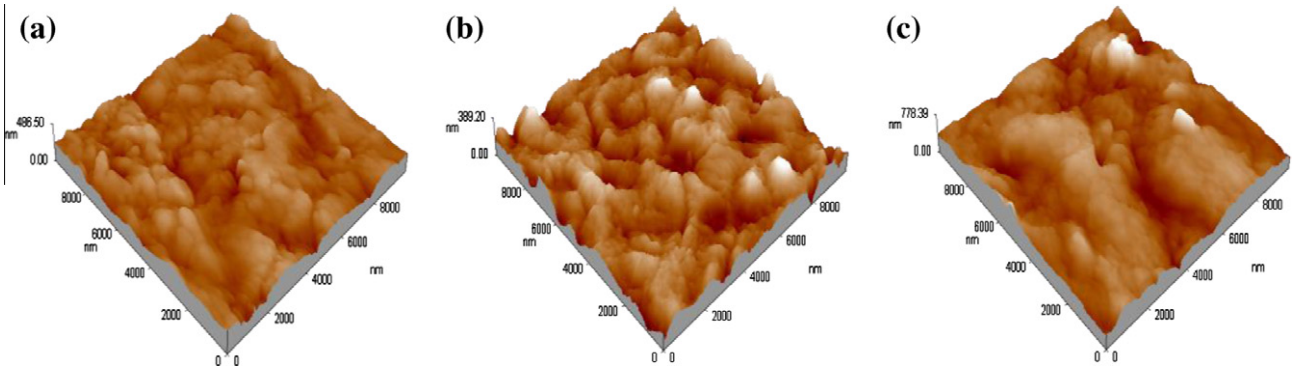

Fig. 4. AFM three-dimensional surface images of membranes: (a) PVDF (b) PVDF/GO and (c) PVDF/MWCNTs.

Table 1
Surface parameters of blend membranes.

Membrane	Surface area (μm^2)	Roughness		
		R_a (nm)	R_q (nm)	R_z (nm)
PVDF	104.45	31.8	40.2	357
PVDF/GO	107.75	40.3	52.2	383
PVDF/MWCNTs	110.68	71.7	91	698

Table 2
Membrane contact angle, porosity and rejection values.

Membrane	Contact angle (°)	Porosity (%)	Rejection (%)
PVDF	80.6 ± 1.7	88.2 ± 1.0	67.6 ± 3.7
PVDF/GO	68.1 ± 2.3	88.8 ± 1.2	87.0 ± 2.3
PVDF/MWCNTs	53.4 ± 2.0	88.7 ± 0.5	89.1 ± 2.1

the surface mean pore size of PVDF/GO membranes was strongly increased, which might play a negative role in BSA rejection. Thereby, the MWCNTs endowed higher rejection for blend membranes than GO.

3.4. Flux of membranes

The effect of carbon materials on the water flux of PVDF blend membranes is shown in Fig. 5. The results indicated that carbon materials led to the increase of the water permeation flux under the feed pressure of 0.1 MPa. Under this pressure differential, the water flux of PVDF/MWCNTs membranes reached a peak value of 620 L m^{-2} h^{-1} and increased approximately 114% compared with the pure membrane. For PVDF/GO blend membranes, 74% improvement of pure water permeation flux was achieved. These findings could be interpreted as that the blend membranes were all endowed with advantageous porous surface and favorable inner structure, which undoubtedly played a positive role in promoting membrane permeability [43]. Furthermore, the addition of MWCNTs and GO resulted in the increase of membrane surface roughness and hydrophilicity (Tables 1 and 2), which might also act favorably in promoting the water permeability. Thus, PVDF/MWCNTs membranes with higher surface roughness and hydrophilicity showed better water permeability compared with PVDF/GO membranes.

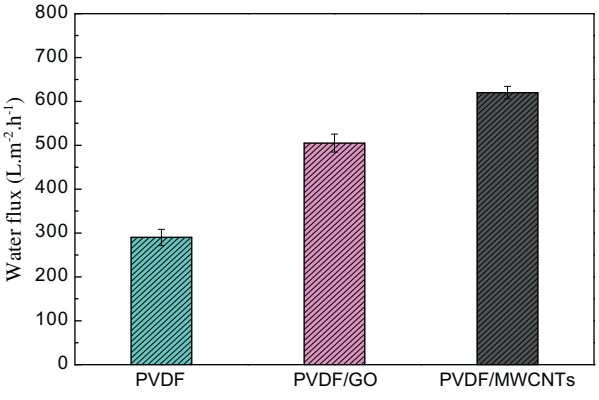

Fig. 5. Pure water flux of membranes.

3.5. Discussion

Owing to the exclusive structures and oxygen groups (such as O—H and COOH, shown in Fig. 1) on the surface of GO and MWCNTs, the blend membranes displayed better surface morphology and performance than pristine ones. It is well known that water permeation flux was strongly determined by the porosity, surface roughness and pore size of membranes [43]. Judging from Table 2, the porosity of PVDF/carbon materials blend membranes was marginally higher than that of pure PVDF membrane. Furthermore, PVDF/GO membranes had bigger pores than the PVDF and PVDF/MWCNTs membranes (Figs. 2 and 3). However, according to Fig. 3 and Table 1, the pore density and surface roughness of PVDF/MWCNTs blend membranes were higher than those of PVDF/GO and PVDF membranes. Thus, these structural differences bring about the difference in membrane water permeation flux.

In addition, the MWCNTs and GO with totally different geometrical structures also provided an important prerequisite for evaluating the effect of material dimensionality on PVDF membrane. As a rigid cylindrical nano-material, one-dimensional MWCNTs with high specific area were regularly collocated in PVDF membrane and forms nodular structure, so the surface of membrane becomes rougher after the addition of MWCNTs. During the phase inversion process, one-dimensional MWCNTs were easy to migrate spontaneously to the membrane/water interface to reduce the interface energy and increase surface hydrophilicity of membranes consequently [23,44]. The migration of MWCNTs to the surface of blend membranes was obvious when surface photographs of prepared membranes were compared as presented in Fig. 2c, which led to further increase in hydrophilicity and surface roughness of PVDF/MWCNTs membranes. But the low specific area and big particle size of three-dimensional GO limit the migration of GO to the membrane surface, resulting in the restricted hydrophilicity and surface roughness of PVDF/GO membranes. For PVDF/GO blend membranes (shown in Fig. 2h), the unconspicuous sponge-like cross-section with floppy inner porous structures may be also attributed to the big three-dimensional particle size and superflu-

Table 3
Comparative results of blend membranes filled with ~1 wt% different inorganic materials.

Membranes	Water flux ($L\ m^{-2}\ h^{-1}$)	Rejection (%)	Contact angle (°)	Reference
PVDF/Al_2O_3	60	96.31	67.87	[10]
PVDF/SiO_2	190	90	78.5	[12]
PVDF/TiO_2	180	90	70.5	[45]
PSF/MWCNTs	60	70	47.5	[29]
PVDF/MWCNTs	620	89.1	53.4	–
PVDF/GO	505	87.0	68.1	–

ous oxygen-containing functional groups of GO which increase the rapid mass transformation between the solvent and non-solvent during the phase inversion. It is demonstrated that MWCNTs with higher specific surface area and moderate oxygen-containing functional groups were more effective in the enhancement of membrane hydrophilicity and permeation than GO. Furthermore, compared with the proportion of inorganic fillers in previous literature, the content of MWCNTs and GO with oxygen-containing functional groups in blend membranes was much lower. As could be seen from Table 3, the PVDF/graphitic carbon material (1 wt%) membranes put up a better performance than the PVDF blend membranes with other inorganic fillers of equal content (1 wt%).

4. Conclusions

PVDF ultrafiltration membranes were synthesized using the phase inversion process, and the effect of graphitic carbon materials on performance of PVDF blend membranes has been investigated. The investigation results were enumerated as below:

(1) The PVDF/graphitic carbon materials blend membranes exhibit better pore structure and higher surface roughness than pure PVDF membrane.
(2) Hydrophilicity of membranes was improved significantly, and the CA of membranes decreased from 80.6° (pure PVDF) to 53.4° (PVDF/MWCNTs) and 68.1° (PVDF/GO). BSA rejection of PVDF/MWCNTs and PVDF/GO blend membranes was enhanced about 31.8% and 28.7% compared with that of pure PVDF membranes, respectively.
(3) Pure water permeation flux of PVDF/MWCNTs and PVDF/GO blend membranes has increased by 114% and 74%, respectively, compared with that of pure PVDF membranes, which was attributed to the high surface roughness as well as the increase of the membrane's porosity and hydrophilicity.
(4) Comparative studies indicated that PVDF/GO blend membranes showed bigger pores but lower pore density and surface roughness and hence performed worse in the hydrophilicity, rejection and pure water permeation flux, compared with PVDF/MWCNTs blend membranes.

It can be expected that graphitic carbon materials open up a new opportunity to improve the performance of blend membranes. And the ultrafiltration membranes modified by graphitic carbon materials have a promising application prospect and also need further investigation to obtain the outstanding performance of blend membranes by surface functionalization, size design and content optimization of graphitic carbon materials.

Acknowledgments

The work was funded by the National Natural Science Foundation of China (11175130), Natural Science Foundation of Tianjin, China (10JCYBJC02300) and China Postdoctoral Science Foundation (20100481092).

References

[1] M.L. Sforca, I.V.P. Yoshida, S.P. Nunes, J. Membr. Sci. 159 (1999) 197–207.
[2] C. Cornelius, C. Hibshman, E. Marand, Sep. Purif. Technol. 25 (2001) 181–193.
[3] X.J. Liu, Y.L. Peng, S.L. Ji, Desalination 221 (2008) 376–382.
[4] Y. Chen, L. Wu, J.Y. Zhu, Y. Shen, S.W. Gan, A.Q. Chen, J. Porous Mater. 18 (2011) 251–258.
[5] B. Tansel, J. Regula, R. Shalewitz, Desalination 102 (1995) 301–311.
[6] S.H. Lin, W.J. Lan, J. Hazard. Mater. 59 (1998) 189–199.
[7] Y.S. Li, L. Yan, C.B. Xiang, L.J. Hong, Desalination 196 (2006) 76–83.
[8] Z. Ademovic, D. Klee, P. Kingshott, R. Kaufmann, H. Hocker, Biomol. Eng. 19 (2002) 177–182.
[9] T. Mohammadi, S.S. Madaeni, M.K. Moghadam, Desalination 153 (2003) 155–160.
[10] L. Yan, Y.S. Li, C.B. Xiang, S. Xianda, J. Membr. Sci. 276 (2006) 162–167.
[11] F. Liu, M.R.M. Abed, K. Li, J. Membr. Sci. 366 (2011) 97–103.
[12] L.Y. Yu, Z.L. Xu, H.M. Shen, H. Yang, J. Membr. Sci. 337 (2009) 257–265.
[13] A.H. Cui, Z. Liu, C.F. Xiao, Y.F. Zhang, J. Membr. Sci. 360 (2010) 259–264.
[14] X.C. Cao, J. Ma, X.H. Shi, Z.J. Ren, Appl. Surf. Sci. 253 (2006) 2003–2010.
[15] S.J. Oh, N. Kim, Y.T. Lee, J. Membr. Sci. 345 (2009) 13–20.
[16] N.L. An, H.Z. Liu, Y.C. Ding, M. Zhang, Y.P. Tang, Appl. Surf. Sci. 257 (2010) 3831–3835.
[17] A. Bottino, G. Capannelli, A. Comite, Desalination 146 (2002) 35–40.
[18] J. Du, L. Wu, C.Y. Tao, C.X. Sun, Acta Phys.-Chim. Sin. 20 (2004) 598–601.
[19] M.L. Yeow, Y.T. Liu, K. Li, J. Membr. Sci. 258 (2005) 16–22.
[20] J.H. Choi, J. Jegal, W.N. Kim, J. Membr. Sci. 284 (2006) 406–415.
[21] H.Q. Wu, B.B. Tang, P.Y. Wu, J. Membr. Sci. 362 (2010) 374–383.
[22] E. Celik, L. Liu, H. Choi, Water Res. 45 (2011) 5287–5294.
[23] E. Celik, H. Park, H. Choi, Water Res. 45 (2011) 274–282.
[24] S.S. Madaeni, S. Zinadini, V. Vatanpour, Sep. Purif. Technol. 80 (2011) 155–162.
[25] J. Heo, H. Kim, N. Her, S. Lee, Y.-G. Park, Y. Yoon, Desalination 298 (2012) 75–84.
[26] E.-S. Kim, G. Hwang, M.G. El-Din, Y. Liu, J. Membr. Sci. 394 (2012) 37–48.
[27] S. Majeed, D. Fierro, K. Buhr, J. Wind, B. Du, A. Boschetti-de-Fierro, V. Abetz, J. Membr. Sci. 403 (2012) 101–109.
[28] V. Vatanpour, S.S. Madaeni, R. Moradian, S. Zinadini, B. Astinchap, Sep. Purif. Technol. 90 (2012) 69–82.
[29] S. Qiu, L.G. Wu, X.J. Pan, L. Zhang, H.L. Chen, C.J. Gao, J. Membr. Sci. 342 (2009) 165–172.
[30] K.S. Novoselov, A.K. Geim, S.V. Morozov, D. Jiang, Y. Zhang, S.V. Dubonos, I.V. Grigorieva, A.A. Firsov, Science 306 (2004) 666–669.
[31] S. Park, D.A. Dikin, S.T. Nguyen, R.S. Ruoff, J. Phys. Chem. C 113 (2009) 15801–15804.
[32] C. Chen, Q.-H. Yang, Y. Yang, W. Lv, Y. Wen, P.-X. Hou, M. Wang, H.-M. Cheng, Adv. Mater. 21 (2009) 3007.
[33] J. Barkauskas, J. Daksevic, R. Juskenas, R. Mazeikiene, G. Niaura, G. Raciukaitis, A. Selskis, I. Stankeviciene, R. Trusovas, J. Mater. Sci. 47 (2012) 5852–5860.
[34] W.H. Kai, Y. Hirota, L. Hua, Y. Inoue, J. Appl. Polym. Sci. 107 (2008) 1395–1400.
[35] D.C. Marcano, D.V. Kosynkin, J.M. Berlin, A. Sinitskii, Z. Sun, A. Slesarev, L.B. Alemany, W. Lu, J.M. Tour, Acs Nano 4 (2010) 4806–4814.
[36] K.C. Khulbe, C. Feng, T. Matsuura, J. Appl. Polym. Sci. 115 (2010) 855–895.
[37] N. Bolong, A.F. Ismail, M.R. Salim, in: International Conference on Advancement of Materials and Nanotechnology, 2010, pp. 358–362.
[38] J.F. Li, Z.L. Xu, H. Yang, Polym. Adv. Technol. 19 (2008) 251–257.
[39] S.T. Yang, J.X. Li, D.D. Shao, J. Hu, X.K. Wang, J. Hazard. Mater. 166 (2009) 109–116.
[40] S. Reza, M. Adeli, B. Astinchap, R. Kabiri, J. Nanopart. Res. 10 (2008) 1309–1318.
[41] L. Palacio, J.I. Calvo, P. Pradanos, A. Hernandez, P. Vaisanen, M. Nystrom, J. Membr. Sci. 152 (1999) 189–201.
[42] Jie Meng, Li Song, Xu Haiyan, Hua Kong, Chaoying Wang, Xiaotian Guo, S. Xie, Nanomed.-Nanotechnol. 1 (2005) 136–142.
[43] P. van der Marel, A. Zwijnenburg, A. Kemperman, M. Wessling, H. Temmink, W. van der Meer, J. Membr. Sci. 348 (2010) 66–74.
[44] M.P. Sun, Y.L. Su, C.X. Mu, Z.Y. Jiang, Ind. Eng. Chem. Res. 49 (2010) 790–796.
[45] Y. Wei, H.Q. Chu, B.Z. Dong, X. Li, S.J. Xia, Z.M. Qiang, Desalination 272 (2011) 90–97.